

Convective precipitation in AROME

Sami Niemelä, FMI

Ulf Andræ, SMHI

Bent Hansen Sass and Bjarne Stig Anderssen, DMI

1 Introduction

FMI, SMHI and DMI have been running both AROME and non-hydrostatic ALADIN with high horizontal resolution (2.5 km) on daily basis for more than a year. This activity has been reported by Sass (2006), Andræ (2005) and Andræ (2006). Performance of these high-resolution models has been evaluated mainly by using traditional verification methods and monthly verification statistics. The main message has been that high-resolution models perform as well as the coarser resolution models (Andræ and Niemelä, 2007).

Where do we expect to gain added value by using km-scale NWP-models? Several studies (e.g., Mass et al., 2002) have addressed this question and have come to the conclusion that it is difficult to extract the additional value when moving from grid scales of about 10 km to km-scale. However, the best possibility to find the value is in prediction of heavy precipitation events and wind structures near meso-scale orographic features (i.e. coastlines, mountains and valleys).

The purpose of this study is to evaluate precipitation forecasts of AROME in two different convective cases. The qualitative assessment concentrates on the general structures (both precipitation and wind) of convective systems. The quantitative evaluation is mainly based on the radar reflectivity data by using the Radar Simulation Model (RSM) of Haase and Crewell (2000). This way we avoid the difficult problem of linking the measured reflectivity to the precipitation at the surface. Previously, RSM has been applied to verification of HIRLAM precipitation (see e.g. Haase and Fortelius, 2001 and Niemelä and Fortelius, 2005). Surface based in-situ precipitation observations from Helsinki Testbed network (Dabberdt et al., 2005) are also used in the comparison.

2 Cases and model setup

Two convective cases were chosen in order to study the quality of the precipitation forecasts of AROME. The first case (10 Jul 2006) includes both Mesoscale Convective Systems (MCS) and a frontal rain band. This study mainly concentrates on the prediction of the MCSs. Figure 1 (top right) shows the observed radar reflectivity 13 UTC 10 Jul 2006. The eastern part of the domain is dominated by rapidly moving (to north-east) MCSs with high precipitation intensities, whereas the western part is widely covered by the frontal rain band moving to east.

The second case (26 Aug 2006) is characterised by small scale convective precipitation with practically no meso-scale organisation. Figure 1 (bottom right) shows the observed radar reflectivity 12 UTC 26 Aug 2006. Most of the Southern Finland is covered by the small scale precipitation cells. In this case the convection is formed in calm wind conditions. Consequently, the convective precipitation cells evolve and decay near the location of their onset.

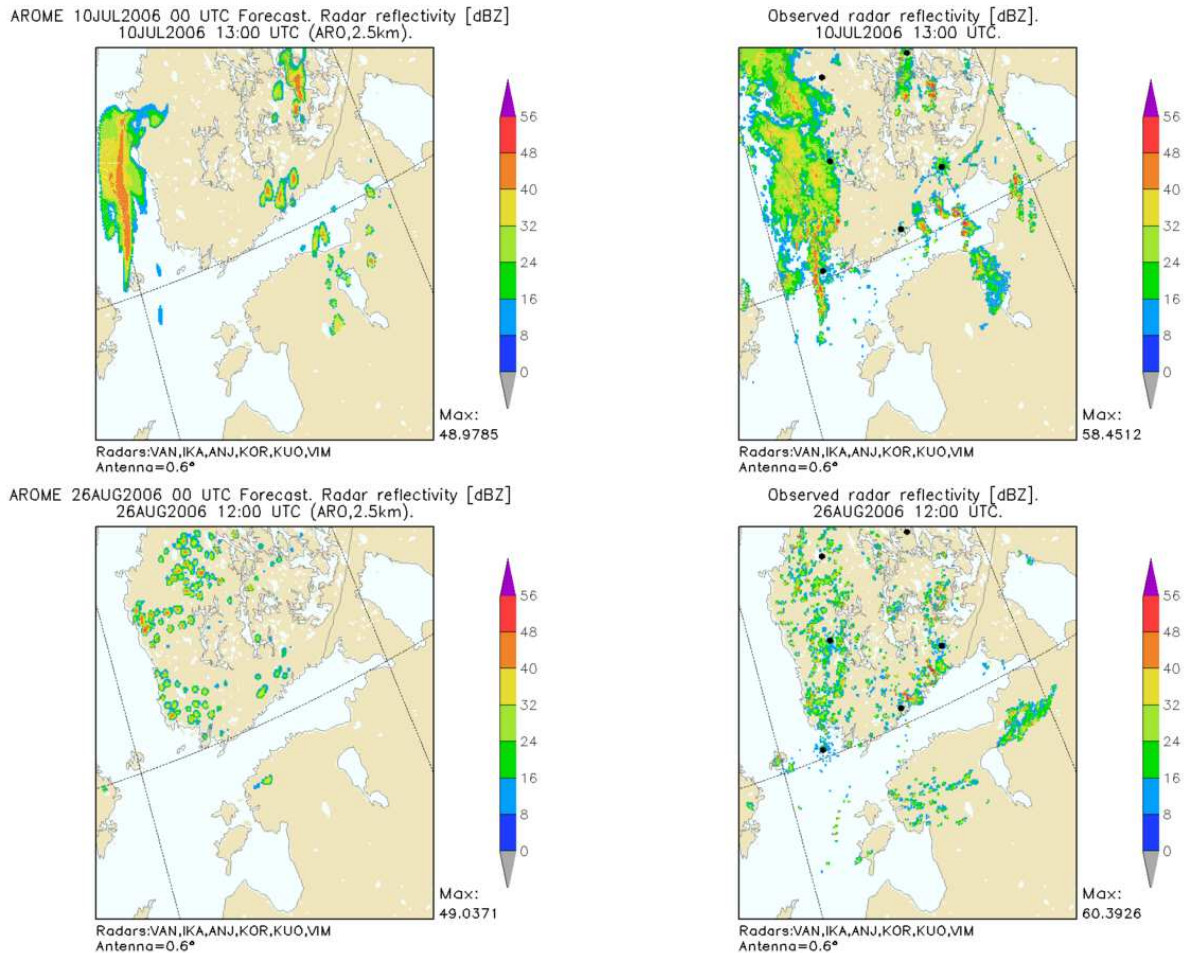


Figure 1: Composite of radar reflectivity [dBZ] fields. Top left: Arome forecast after 13 hour forecast valid at 13 UTC 10 Jul 2006. Top right: radar observation at 13 UTC 10 Jul 2006. Bottom left: Arome forecast after 12 hour forecast valid at 12 UTC 26 Aug 2006. Bottom right: radar observation at 12 UTC 26 Aug 2006. The locations of the radars are marked with black dots.

FMI's daily AROME suite is based on the CY30T1. The horizontal resolution is 2.5 km with 40 vertical levels. 24 hour forecast is conducted twice a day with 60 s time step. It should be emphasised that this implementation of AROME neither use the deep convection parameterization nor mesoscale data assimilation. The initial state and the outer boundaries are taken from FMI's operational HIRLAM-RCR (22 km). First, the HIRLAM-RCR forecasts are downscaled by ALADIN (11 km) model, which is further downscaled by AROME.

3 Results

3.1 Case 1: 10 July 2006

Top panels in Fig. 1 illustrate forecasted (left) and observed (right) reflectivity field after 13 hour model integration. AROME is able to create realistically looking MCS structures over the region where they really occur. Naturally, the individual cells are not predicted exactly at right location. AROME is also able to form a rain band, which seems to be too intense (>32 dBZ) over too large area. The rain band is also delayed significantly most likely due to the closeness of the model boundary. Therefore, we concentrate on the region of MCS activity.

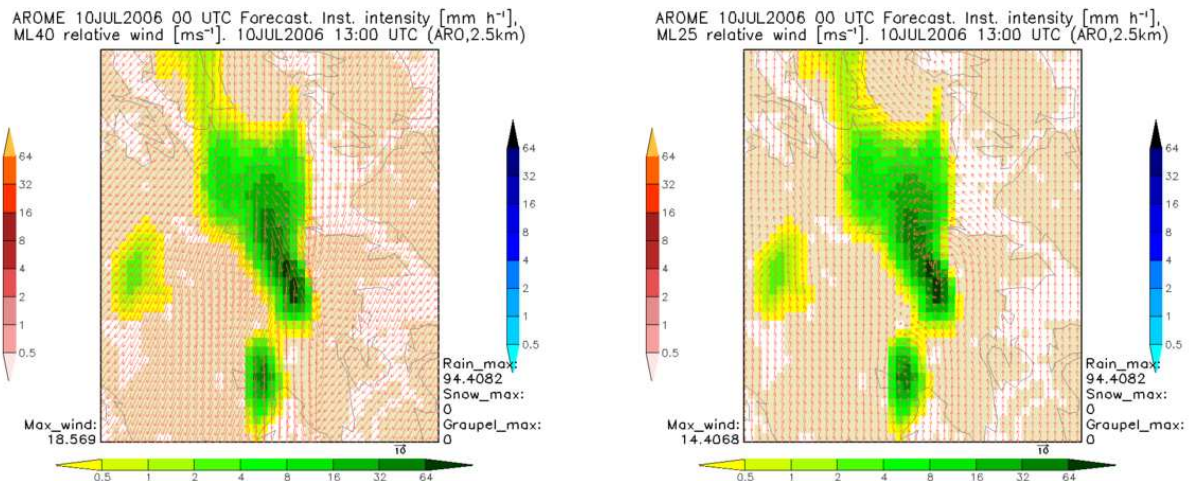


Figure 2: Instantaneous precipitation intensity at surface [mm h⁻¹] and wind vectors at height of 30 m (left) and 3000 m (right) after 13 hour forecast. Wind is presented as vectors relative to the movement of the MCS. The MCS is moving to north-east.

What kind of structures we can expect to see in a MCS? Figure 2 shows detailed structure of one individual convective system predicted by AROME. The wind vectors describe the relative wind related to movement of the MCS at height of 30 m (left) and 3000 m (right). The relative wind structure near the surface includes rear and front *outflow* away from the system. The front outflow collides with inflow creating a 'gust front' in front of the MCS. Higher above (3000 m) both front and rear *inflows* are present, generating the convergence line in the middle of the MCS. This is the region of most intense precipitation. The model results correspond qualitatively the structures of classical multicell thunderstorm presented by Browning et al. (1976).

Figure 3 (left) presents frequency distribution of radar reflectivity from the case 1. The focus is on the area of the most intense MCS activity. The most important finding is the overestimation of moderate and strong reflectivities (between 28 and 44 dBZ). AROME tends to produce too large MCSs with too intense precipitation. Another interesting feature is the underestimation of the strongest echoes (>44 dBZ). In this case, very large hails were detected causing the strongest values. It is encouraging that AROME does not create such a high values, since the prognostic hail treatment is not present in this version of the model. The underestimation of the weak reflectivities (<20 dBZ) is not so important since such dBZ-values correspond the rain intensity less than 0.5 mm h⁻¹.

3.2 Case 2: 26 August 2006

Panels below in Fig. 1 illustrate forecasted (left) and observed (right) reflectivity field after 12 hour model integration. Again AROME model is able to form realistically looking small scale convective cells, especially on the western part of the Finland. Figure 3 (right) shows frequency distribution of the reflectivities when convective activity was present both in model and in reality. This time there is only a slight indication of the overestimation of the moderate and strong reflectivities. The strongest reflectivities are again underestimated. In this case, AROME is not able to capture the only organised system present in the southern coast of Finland. This small system caused the strongest echoes.

Figure 4 shows the time series of the reflectivity frequency bias with the threshold range between 16–70 dBZ. This score gives information about the areal coverage of the precipitation. The convection starts at 9 UTC (12 LT). The onset in AROME is roughly delayed by 1 hour. It takes nearly 2 hours (10–12 UTC) to catch up the reality. During the mature and decaying state (12–18 UTC) the areal extent of the precipitation is very well represented by AROME. Also the end of the convection is timed correctly (19 UTC)

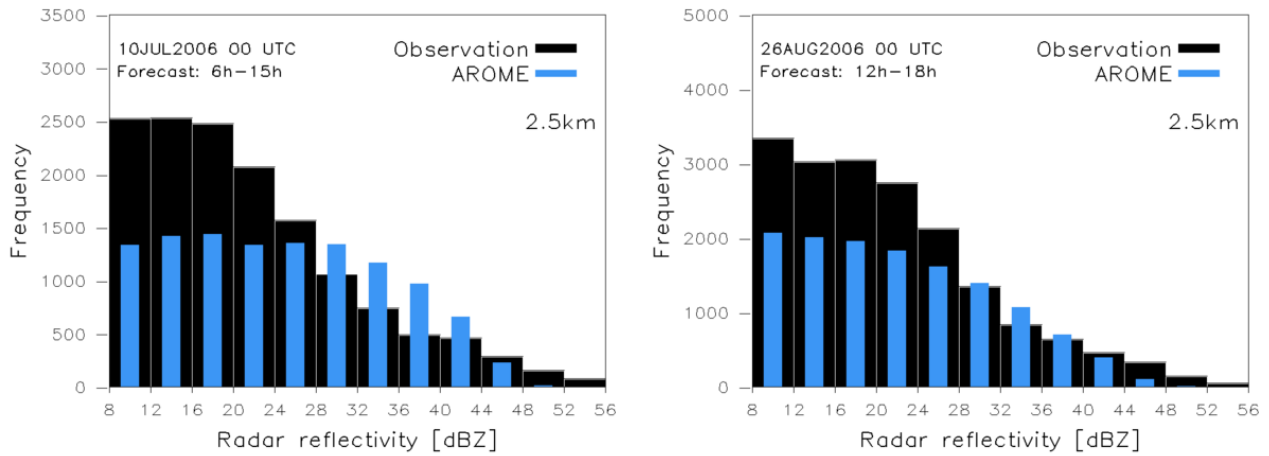


Figure 3: Frequency distribution of radar reflectivity [dBZ]. AROME forecast is represented with blue bars, whereas black bars represent dBZ-observations. The radar antenna elevation is 0.6°. Left: 10 July 2007, distribution is from the area of the most intense MCS activity (eastern part of the domain in top panels of Fig. 1). Right: 26 August 2006.

So far, the quantitative assessment has involved the radar data only. From the forecasting point of view, the precipitation at the surface is the more important parameter. Figure 5 compares the frequency distributions of 3h-accumulated precipitation produced by AROME and FMI’s operational 9 km HIRLAM during the 25–27 August 2006. This period was characterised by similar small scale convection as presented in case 2. It is clear that HIRLAM overestimates all the precipitation classes, whereas AROME reproduces the observed distribution well. HIRLAM spreads the precipitation all over the southern Finland (not shown). Evidently a 9 km grid-size is not small enough to capture the structures of this small scale convection.

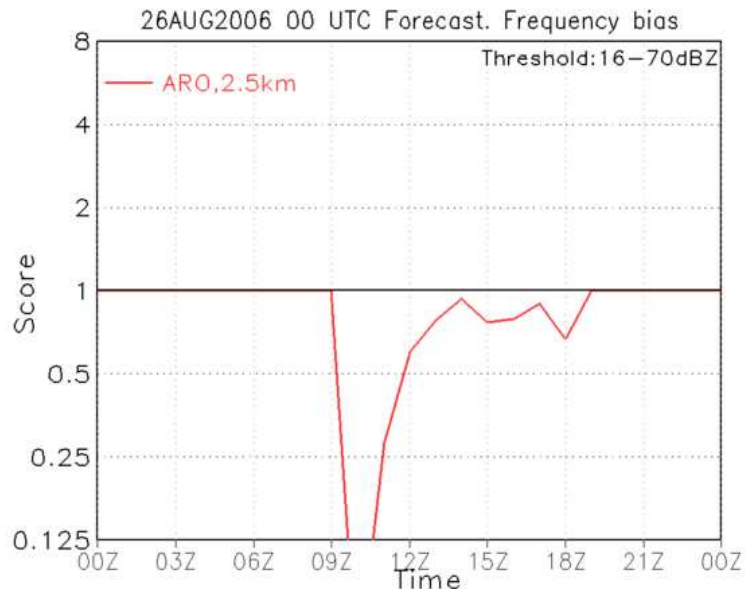


Figure 4: Time series of reflectivity frequency bias (ratio between forecasted and observed occurrence). The radar antenna elevation is 0.6°.

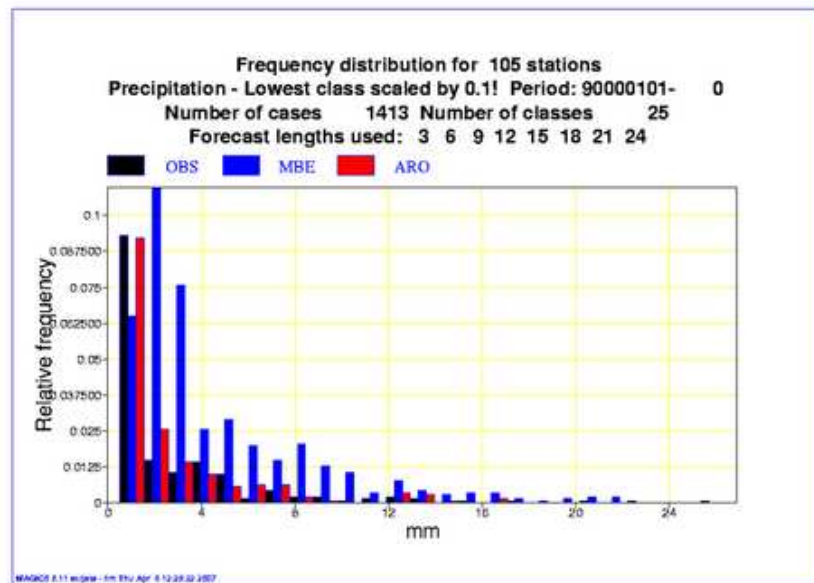


Figure 5: Frequency distribution of 3h-accumulated precipitation during 25–27 August 2006. Red bars represent AROME (2.5 km) and blue bars HIRLAM (FMI’s operational model with 9 km horizontal resolution) forecasts, respectively. Black bars show the observed distribution taken from the Helsinki Testbed measurement network. (Dabberdt et al., 2005)

4 Conclusions

This paper presented both qualitative and quantitative assessment of the AROME precipitation forecasts in two different convective cases. The findings of the study can be summarised as follows.

- AROME is able to create qualitatively realistic MCS structures and weakly forced convective cells.
- There is an indication that AROME is overestimating moderate and strong reflectivities (i.e. precipitation intensity). This might be a sign that the model is forcing convection to occur in too large scale.
- In weakly forced case, the onset of convection is delayed by 1 hour. However, the end of the convection is well predicted.
- In case of the small scale convection, km-scale AROME can produce better precipitation distribution than 9 km HIRLAM model.

References

- Andræ, U., 2005: Daily runs with ALADIN at SMHI. *HIRLAM newsletter*, **49**, 89–104. Available from <http://hirlam.org/open/publications/NewsLetters/>.
- Andræ, U., 2006: SMHI ALADIN implementation. *HIRLAM newsletter*, **51**, 36–57. Available from <http://hirlam.org/open/publications/NewsLetters/>.
- Andræ, U. and S. Niemelä, 2007: Daily runs with ALADIN/AROME. HIRLAM all-staff meeting/ALADIN workshop, Oslo, Norway, 23–26 Apr, 2007. Available online at http://hirlam.org/open/meetings/ASM2007/s2_andrae.pdf.

- Browning, K. A., J. C. Frankhauser, J.-P. Chalon, P. J. Eccles, R. G. Strauch, F. H. Merrem, D. J. Musil, E. L. May and W. R. Sand, 1976: Structure of an evolving hailstorm part V: Synthesis and implications for hail growth and hail suppression. *Mon. Wea. Rev.*, **104**(5), 603–610.
- Dabberdt, W., J. Koistinen, J. Poutiainen, E. Saltikoff and H. Turtiainen, 2005: The Helsinki mesoscale Testbed - An invitation to use a new 3-D observation network. *Bull. Amer. Met. Soc.*, **86**(7), 906–907.
- Haase, G. and S. Crewell, 2000: Simulation of radar reflectivities using a mesoscale weather forecast model. *Water Resour. Res.*, **36**, 2221–2231.
- Haase, G. and C. Fortelius, 2001: Simulation of radar reflectivities using Hirlam forecasts. HIRLAM Tech. Rep. 51, SMHI, S-601 76 Norrköping, Sweden. Hirlam-5 Project, 22 pp. [available online at <http://hirlam.org/open/publications/TechReports/>].
- Mass, C. F., D. Ovens, K. Westrick and B. A. Colle, 2002: Does increasing horizontal resolution produce more skillful forecasts? *Bull. Am. Meteor. Soc.*, **83**, 407–430.
- Niemelä, S. and C. Fortelius, 2005: Applicability of large-scale convection and condensation parameterization to meso- γ -scale HIRLAM: a case study of a convective event. *Mon. Wea. Rev.*, **133**(8), 2422–2435.
- Sass, B. H., 2006: A short summary of the HIRLAM work on IFS/ALADIN during mesoscale project 2004–2006. *HIRLAM newsletter*, **51**, 33–35. Available from <http://hirlam.org/open/publications/NewsLetters/>.